Electronic and magnetic properties of embedded Rh clusters in Ni matrix

1995 J. Phys.: Condens. Matter 7 7367

(http://iopscience.iop.org/0953-8984/7/37/009)

J. Phys.: Condens. Matter 7 (1995) 7367–7372. Printed in the UK

Electronic and magnetic properties of embedded Rh clusters in Ni matrix

Zhi-Qiang Li†, Yuichi Hashi‡, Jing-Zhi Yu†, Kaoru Ohno† and Yoshiyuki Kawazoe†

† Institute for Materials Research, Tohoku University, Sendai 980-77, Japan
‡ Hitachi Tohoku Software Ltd, Research and Development Centre, Sendai 980, Japan

Received 20 March 1995, in final form 22 May 1995

Abstract. The electronic structure and magnetic properties of rhodium clusters with sizes of one to 43 atoms embedded in a nickel host are studied by first-principles spin-polarized calculations within the local density functional formalism. A single Rh atom in Ni matrix is found to have a magnetic moment of 0.45 μ_B. Rh_{13} and Rh_{19} clusters in Ni matrix have lower magnetic moments compared with the free ones. The most interesting finding is that Rh_{43} cluster, which is bulk-like and non-magnetic in vacuum, becomes ferromagnetic when embedded in the nickel host.

Atomic clusters have opened new prospects in the development of materials science. Taking advantage of the characteristic behaviour of small particles, one expects to be able to tailor new materials for specific technological purposes. Consequently, much effort has been invested in the research on the properties of microclusters [1]. Rhodium has specially interesting magnetic properties. It is non-magnetic in the bulk state. However, the rhodium monolayers on an iron substrate have a measured magnetic moment of 0.82 μ_B per atom [6]. Since Reddy *et al* [2] predicted that small rhodium clusters would show ferromagnetic properties, many experimental and theoretical investigations have been conducted to explore the unusual magnetic properties of rhodium clusters [3, 4, 5].

Using the local spin density (LSD) functional theory, Reddy *et al* [2] recently calculated the magnetic moments for ruthenium, rhodium, and palladium 13-atom clusters with icosahedral and cubo-octahedral symmetry. They predicted moments of 1.62 μ_B per atom for icosahedral Rh_{13}, 1.02 μ_B per atom for icosahedral Ru_{13}, and 0.12 μ_B for icosahedral Pd_{13}. Indeed, Cox *et al* [3] observed experimentally giant magnetic moments in small Rh_n clusters with $n = 12$–34. However, their observed value of the average magnetic moment per atom for Rh_{13} is 0.48 μ_B, only about one-third of the theoretical prediction of Reddy *et al*. They also found that the average moment per atom of the Rh clusters depends significantly on the cluster size. There are several sizes, Rh_{15}, Rh_{16}, and Rh_{19} which have magnetic moments per atom that are significantly larger than those of adjacent cluster sizes. The average moment of the rhodium cluster decreases to the bulk value of zero as the cluster size increases. Yang *et al* [4] have also performed first-principles studies on Rh_n ($n = 2$–19) clusters, and they did not observe the magnetic transition from magnetic state to non-magnetic state as the cluster size increases, due to the small number of atoms in their studies.

We have studied the electronic structure and magnetic properties of Rh_n ($n = 6$, 9, 13, 19, 43) clusters and obtained better results compared with the experiments [5]. Moreover,

0953-8984/95/377367+06$19.50

we found that the magnetic and electronic structure of the Rh_{43} cluster have almost the same features as that of the rhodium bulk.

For most technological applications, the properties of embedded clusters (e.g. clusters in a matrix) are more relevant than free clusters because they are related to the granular or island geometrical arrangements observed in overlayers, sandwiches, and multilayers. Therefore, it is of considerable importance to extend our knowledge on free clusters to the cases where these clusters are embedded in an environment. Comparison between the behaviour of the free and embedded clusters would also contribute significantly to the understanding of the specific properties of these materials.

The formation of a magnetic moment on isolated transition metal impurities dissolved into metallic hosts continues to be a topic of experimental as well as theoretical interest. Extensive data are now available for the magnetism of 3d ions in various metals [7]. In comparison, much less information is available on the magnetic behaviour of isolated 4d impurities in transition metal hosts. Using a cluster model, we can study the magnetic impurities in a more flexible way.

As an extension to our previous paper on free rhodium clusters, we report here a first-principles study on Rh_n clusters embedded in a nickel matrix. We chose nickel as host because it has the same fcc structure as rhodium and it is ferromagnetic. The Ni_{43} cluster is used as a model of the nickel matrix, as we will discuss later, which represents well the electronic and magnetic structures of nickel crystal within the local spin-density (LSD) formalism [8].

The electronic structures of the clusters are calculated with the first-principles discrete variational method (DVM) [10]. The same method has already been employed in several other studies on metal clusters [11, 12], and described in detail elsewhere [12]. In short, the numerical atomic orbitals are used in the construction of molecular orbitals. In the present work, atomic orbital configurations composed of 4d, 5s and 5p for Rh and 3d, 4s and 4p for Ni are employed to generate the valence orbitals. The secular equation $(H - ES)C = 0$ is then solved self-consistently using the matrix elements obtained via three-dimensional numerical integrations on a grid of random points by the Diophantine method. About 900 sampling points around each site are employed. These points were found to be sufficient for convergence of the electronic spectrum within 0.01eV [11]. The self-consistent charge (SCC) scheme [13] and von Barth–Hedin [9] exchange–correlation function are used in the calculations. In recent years, the inclusion of the gradient corrections to the LSD functionals has made a great advance in the description of molecules and solids, especially for the energetics, i.e. the binding energy or cohersive energy [14, 15, 16]. The so called non-local spin density (NLSD) theory gives the correct ground bcc ferromagnetic state of iron, for which LSD gets the wrong paramagnetic fcc lattice. However, it has no improvements over LSD on the magnetic moments, as compared with experiments [16]. The justification of the present calculation method has been demonstrated in many publications [2, 4, 5, 21].

We first study the Ni_{43} cluster in the fcc structure with the lattice constant of nickel bulk, see figure 1, which is used as a model of nickel bulk. There are four different sites in this cluster labelled A–D. The calculated results are summarized in table 1. The central atom in the model (A site) has the lowest magnetic moment of 0.66 μ_B which is in good agreement with the value of nickel bulk. It is noted that while the 3d moment is positive, the 4s and 4p moments are negative. The local density of states (DOS) of the central atom in this cluster is shown in figure 2, which is obtained by a Lorentz expansion of the discrete energy levels and a summation over them. In comparison with the DOS of nickel bulk calculated by the LDA band-structure method [18], we notice that the main features, namely three large peaks and about 4 eV valence band width, are well reproduced by the

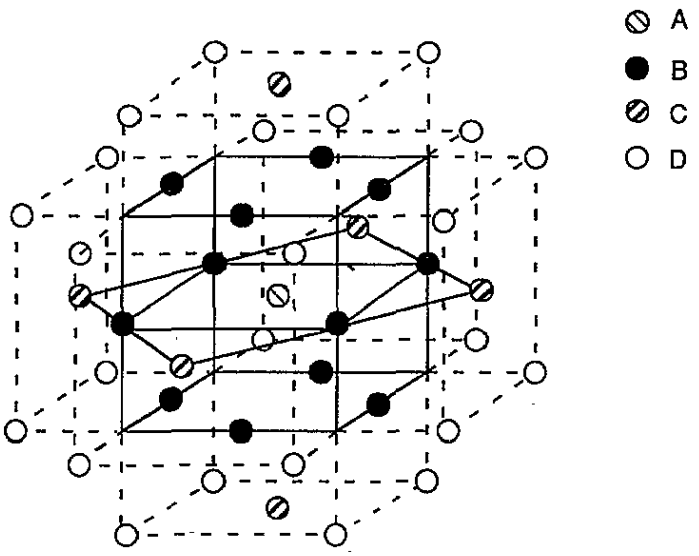

Figure 1. Structure of cluster model, different sites are labelled by A–D.

Table 1. Magnetic moments of each site of Ni_{43} and $RhNi_{42}$ clusters.

	A	B	C	D
Ni_{43}				
d	0.73	0.74	0.97	1.10
s	−0.03	−0.02	−0.03	0.03
p	−0.04	−0.01	−0.05	−0.01
Total	0.66	0.71	0.89	1.12
$RhNi_{42}$				
d	0.55	0.64	0.98	1.08
s	−0.03	−0.02	−0.03	0.02
p	−0.07	0.01	−0.06	−0.02
Total	0.45	0.63	0.89	1.08

Ni_{43} clusters. Therefore, this cluster can be used to represent the nickel bulk for dealing with the local problems.

Next, we discuss the local moment formation of a single Rh impurity in an Ni host. Zeller [19] has examined the electronic structure of 4d impurities in Ni, using a LSD approach based on the Korringa–Kohn–Rostoker (KKR) Green function method. Here the impurity is described by a single-site perturbated muffin-tin potential in an otherwise perfect periodic lattice. The calculated magnetic moment of the Rh atom is 0.57 μ_B which is much smaller than the experimental result of 2 μ_B observed by neutron scattering [20]. However, this experimental result is contrary to the expectation that in the 4d series the moments are always smaller than the 3d series and therefore the Rh moment should be smaller than the Co moment of 1.8 μ_B.

The discrepancy between the theory and experiment is so large that it deserves more studies by different approaches. Here, we use a cluster model to represent one Rh impurity in the Ni host. A similiar approach has been used to calculate the magnetism of a single Fe impurity in Al by a 43-atom cluster [21]. The calculated results are listed in table 1. The total magnetic moment of Rh atom is 0.45 μ_B which mainly arises from the polarization

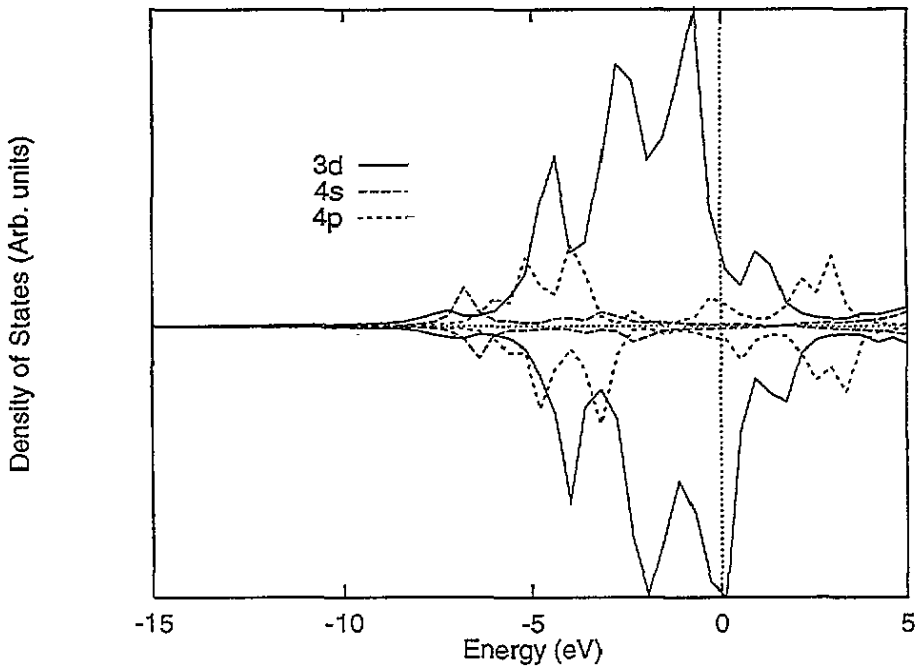

Figure 2. Local density of states of the central atom in the Ni_{43} cluster.

of d states whereas s and p polarization add only a small negative contribution. It is noted from table 1 that the effect of the Rh impurity on the Ni host is quite local, with only a little change for the next-nearest-neighbouring Ni atoms. Our result is in good agreement with the KKR calculations but contrary to the neutron scattering experiments. A possible reason for the discrepancy may be the analysis of the experiments. The experimentalist uses a two-moment version of the local environment model and the application is incomplete as has been argued by Hicks [22].

Table 2. Magnetic moments of Rh_n and Rh_nNi_{43-n} clusters at different sites A–E.

Cluster	A	B	C	D	E
Rh_{13}	1.59	0.63			
Rh_{19}	0.06	0.59	0.16		
Rh_{43}	0.00	0.13	0.04	0.01	
Ni_{43}	0.66	0.71	0.89	1.12	
$RhNi_{42}$	0.45	0.63	0.89	1.08	
$Rh_{13}Ni_{30}$	0.49	0.52	0.99	1.11	
$Rh_{19}Ni_{24}$	0.25	0.37	0.21	1.24	
$Rh_{43}Ni_{12}$	0.02	0.23	0.35	0.53	1.45

Figure 3 shows the LDOS of the Rh atom in the nickel host. It is clear that small exchange splitting between the majority and minority spin results in the magnetic formation of the Rh atom. Compared with the LDOS of the free Rh_{43} cluster, it is noticed there are extra states for both majority and minority spin at about −7 eV below the Fermi level, which are due to the hybridization of Ni 3d and Rh 4d states.

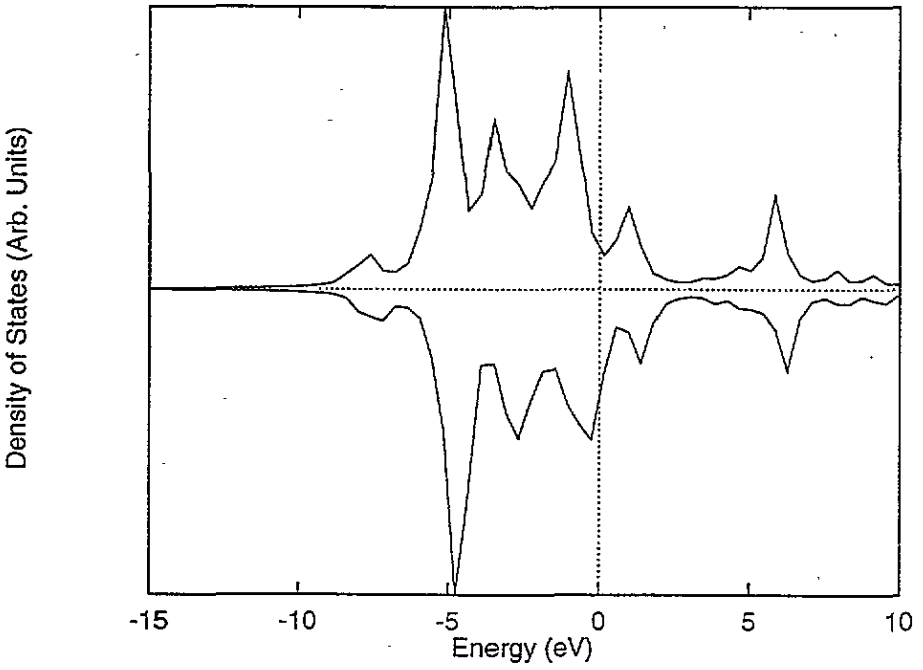

Figure 3. Local density of states of the Rh atom in the $RhNi_{42}$ cluster.

In the previous paper [5], we have shown that small rhodium clusters have finite magnetic moments, and the Rh_{43} cluster is non-magnetic exhibiting bulk-like electronic and magnetic properties. To characterize the effect of the matrix on the magnetic moments of Rh clusters, we study the electronic properties of Rh_nNi_{43-n} and $Rh_{43}Ni_{12}$ clusters. The interatomic distances for Rh–Rh and Ni–Ni are these of the corresponding bulk, while the interatomic distance for Rh–Ni is the average of the Ni and Rh bulk. The lattice constants of Ni and Rh are 3.524 Å and 3.804 Å respectively.

Table 2 gives the calculated magnetic moments for each cluster as well as the results of free clusters for comparison. The embedded Rh_{13} and Rh_{19} clusters are also ferromagnetic with reduced magnetic moments compared with the free ones. It is interesting to note that the Rh_{19} cluster surrounded by Rh_{24} is bulk-like non-magnetic, whereas it is ferromagnetic when surrounded by Ni_{24}. To further clarify this point, we study a larger cluster $Rh_{43}Ni_{12}$, which has 12 nickel atoms surrounding a 43-Rh cluster in the fcc structure. We find that the Rh_{43} cluster becomes ferromagnetic in this case. This is very similar to the experimental observation that a rhodium monolayer over iron has a magnetic moment which is induced by the hybridization of 4d–3d electronic states [6]. Therefore, one can obtain larger ferromagnetic Rh clusters in this way and we hope that experiments may check our expectation.

From table 2 it is noted that the magnetic moments of Ni atoms in $Rh_{19}Ni_{24}$ and $Rh_{43}Ni_{12}$ clusters are a little bit larger. This is due to the fact that these atoms are at the surface of the clusters and the next inner shell is Rh. As we mentioned above, we used the average interatomic distance of Ni–Ni and Rh–Rh in the bulk as the interatomic distance of Ni–Rh in the cluster. Therefore, the bondlengths between a Ni atom at the surface and a Rh atom at the inner shell of the cluster are longer, which results in the larger Ni magnetic moments

in these two cases.

To summarize, by using the first-principles self-consistent LSD calculations, we find that a single Rh atom impurity in the Ni host has a magnetic moment of 0.45 μ_B and the embedded Rh_{13} and Rh_{19} clusters are also ferromagnetic though the moments are smaller than the free clusters. While the free-standing Rh_{43} cluster shows the non-magnetic property, the embedded one has induced magnetic moments. Those properties might be found in granular materials and thin films.

Acknowledgments

The authors would like to express their sincere thanks to the Materials Information Science Group of the Institute for Materials Research, Tohoku University, for their continuous support of the HITAC S3800/380 supercomputing facilities.

References

[1] See
Proc. 6th Int. Meeting on Small Particles and Inorganic Clusters (Chicago, 1992) 1993 Z. *Phys.* D **26**
[2] Reddy B V, Khanna S N and Dunlap B I 1993 *Phys. Rev. Lett.* **70** 3323
[3] Cox A J, Louderback J G, Apsel S E and Bloomfield L A 1993 *Phys. Rev. Lett.* **71** 923; 1994 *Phys. Rev.* B **49** 12 295
[4] Yang Jinlong, Toigo F, Wang Kelin 1994 *Phys. Rev.* B **50** 7915
[5] Li Z Q, Yu J Z, Ohno K and Kawazoe Y 1995 *J. Phys.: Condens. Matter* **7** 47
[6] Kachel T and Gudat W 1992 *Phys. Rev.* B **46** 12 888
[7] Fisher K H 1982 *Landolt–Börnstein: Numerical Data and Functional Relationship in Science and Technology* ed K H Hellwege and J L Olsen (Berlin: Springer)
[8] Kohn W and Sham L J 1965 *Phys. Rev.* A **140** 1133
[9] von Barth U and Hedin L 1972 *J. Phys. C: Solid State Phys.* **5** 1629
[10] Delley B, Ellis D E, Freeman A J and Post D 1983 *Phys. Rev.* B **27** 2132
[11] Press M R, Liu F, Khanna S N and Jena P 1989 *Phys. Rev.* B **40** 399
[12] Li Z Q and Gu B L 1993 *Phys. Rev.* B **47** 13 611
[13] Ellis D E and Painter G P 1970 *Phys. Rev.* B **2** 2887
[14] Perdew J P, Chevary J A, Vosko S H, Jackson K A, Perdersion M R, Singh D J and Fiolhais C 1992 *Phys. Rev.* B **46** 6671 and references therein
[15] Kutzler F W and Painter G S 1992 *Phys. Rev.* B **46** 3236
[16] Singh D J, Pickett W E and Krakauer H 1991 *Phys. Rev.* B **43** 11 628
[17] Zhu J, Wang X W and Louie S G 1992 *Phys. Rev.* B **45** 8887
[18] Moruzzi V L, Janak J F and Williams A R 1978 *Calculated Electronic Properties of Metals* (New York: Pergamon)
[19] Zeller R 1987 *J. Phys. F: Met. Phys.* **17** 2123
[20] Cable J W 1977 *Phys. Rev.* B **15** 3477
[21] Guenzburger D and Ellis D E 1991 *Phys. Rev. Lett.* **67** 3832; 1992 *Phys. Rev.* B **45** 285
[22] Hicks T J 1980 *J. Phys. F: Met. Phys.* **10** 879